Description of the "TRIFFID" Dynamic Global Vegetation Model

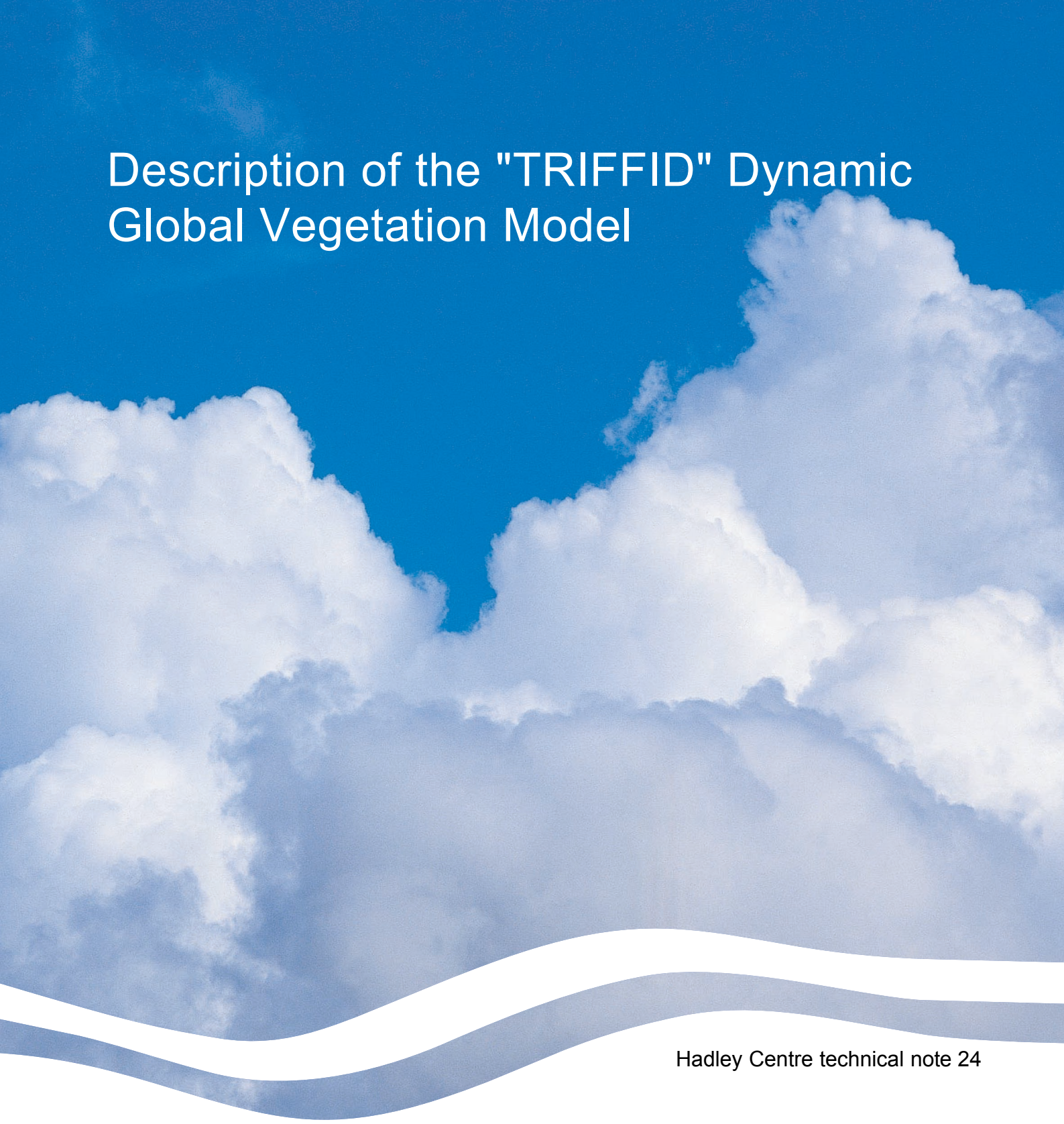

Hadley Centre technical note 24

Peter M. Cox

Hadley Centre, Met Office, London Road, Bracknell, Berks, RG122SY, UK

17 January 2001

Description of the "TRIFFID" Dynamic Global Vegetation Model

Peter Cox

Hadley Centre, Met Office, London Road, Bracknell, Berks R12 2SY, UK
pmcox@meto.gov.uk

January 17, 2001

Abstract

This note describes the terrestrial carbon cycle component of the Hadley Centre's coupled climate-carbon cycle model (Cox *et al* (2000)). "TRIFFID (Top-down Representation of Interactive Foliage and Flora Including Dynamics)" is a dynamic global vegetation model, which updates the plant distribution and soil carbon based on climate-sensitive CO_2 fluxes at the land-atmosphere interface. The surface CO_2 fluxes associated with photosynthesis and plant respiration are calculated in the MOSES 2 tiled land-surface scheme (Essery *et al* (In preparation)), on each atmospheric model timestep (normally 30 minutes), for each of 5 plant functional types. The area covered by a plant type is updated (normally every 10 days) based on the net carbon available to it and on the competition with other plant types, which is modelled using a Lotka-Volterra approach. Soil carbon is increased by litterfall, which can arise from local processes such as leaf-drop as well as large-scale disturbances which reduce the vegetated area. Soil carbon is returned to the atmosphere by microbial respiration which occurs at a rate dependent on soil moisture and temperature. TRIFFID has been designed to allow economical diagnosis of initial states using a Newton-Raphson descent towards the equilibrium state consistent with a given climate.

1 Introduction

Over the last decade a number of groups have developed equilibrum biogeography models which successfully predict the global distribution of vegetation based on climate (Prentice *et al* (1992), Woodward *et al* (1995)). Such models have been coupled "asynchronously" to GCMs in order to quantify climate-vegetation feedbacks. This involves an iterative procedure in which the GCM calculates the climate implied by a given landcover, and the vegetation model calculates the landcover implied by a given climate. The process is repeated until a mutual climate-vegetation equilibrium is reached (Claussen (1996)), Betts *et al* (1997)). Such techniques have yielded very interesting results but suffer from two main limitations. Firstly, such asynchronous coupling may hide inconsistencies since the climate model and the vegetation model can represent common processes (such as the surface water balance) in different ways. This can lead to a mismatch between the variables and fluxes calculated in each. The second limitation is due to the implicit assumption that the climate and vegetation are in an equilibrium state. Although this may be an reasonable assumption for studying different vegetation-climate states on the timescales of interest in palaeoclimate modelling (Claussen (1996)), it is not appropriate for simulating transient climate change over the next century, during which time the terrestrial biosphere is likely to be far from an equilibrium state.

In order to fully understand the role of climate-vegetation feedbacks on these timescales we need to treat the landcover as a interactive element, by incorporating dynamic global vegetation models (DGVMs) directly within climate models. The earliest DGVMs were based on bottom-up "gap" forest models, which explicitly model the growth, death and competition of individual plants (Friend *et al* (1993); Post and Pastor (1996)). Such models can produce very detailed predictions of vegetation

responses to climate, but they are computationally expensive for large-scale applications. Also, GCM climates are not likely to be sensitive to the details of the species or age composition of the landcover. For this study it is more appropriate to adopt a "top-down" DGVM approach, in which the relevant land-surface characteristics, such as vegetated fraction and leaf area index, are modelled directly (Foley *et al* (1996)). A model of this type, called "TRIFFID" ("Top-down Representation of Interactive Foliage and Flora Including Dynamics"), has been developed at the Hadley Centre for use in coupled climate-carbon cycle simulations (Cox *et al* (2000)).

2 Coupling to the GCM Land-Surface Scheme

TRIFFID defines the state of the terrestrial biosphere in terms of the soil carbon, and the structure and coverage of five plant functional types (Broadleaf tree, Needleleaf tree, C_3 grass, C_4 grass and shrub). The areal coverage, leaf area index and canopy height of each PFT are updated using a "carbon balance" approach, in which vegetation change is driven by net carbon fluxes calculated within the "MOSES 2" land surface scheme. MOSES 2 is a "tiled" version of the land surface scheme described by Cox *et al* (1999), in which a separate surface flux and temperature is calculated for each of the landcover types present in a GCM gridbox. In its standard configuration, MOSES 2 recognises the five TRIFFID vegetation types plus four non-vegetation landcover types (bare soil, inland water, urban areas and land ice). Carbon fluxes for each of the vegetation types are derived using the coupled photosynthesis-stomatal conductance model developed by Cox *et al* (1998), which utilises existing models of leaf-level photosynthesis in C_3 and C_4 plants (Collatz *et al* (1991), Collatz *et al* (1992)). Full details of this part of MOSES 2 are given in appendix A. The resulting rates of photosynthesis and plant respiration are dependent on both climate and atmospheric CO_2 concentration. Therefore, with this carbon-balance approach, the response of vegetation to climate occurs via climate-induced changes in the vegetation to atmosphere fluxes of carbon.

Figure 1 is a schematic showing how the MOSES 2 land-surface scheme is coupled to TRIFFID for each vegetation type. The land-atmosphere fluxes (above the dotted line) are calculated within MOSES 2 on every 30 minute GCM timestep and time-averaged before being passed to TRIFFID (usually every 10 days). TRIFFID (below the dotted line of figure 1) allocates the average net primary productivity over this coupling period into the growth of the existing vegetation (leaf, root and wood biomass), and to the expansion of the "vegetated area". Leaf phenology (bud-burst and leaf drop) is updated on an intermediate timescale of 1 day, using accumulated temperature-dependent leaf turnover rates. After each call to TRIFFID the land surface parameters required by MOSES 2 (e.g. albedo, roughness length) are updated based on the new vegetation state, so that changes in the biophysical properties of the land surface, as well as changes in terrestrial carbon, feedback onto the atmosphere (figure 2). The land surface parameters are calculated as a function of the type, height and leaf area index of the vegetation, as described in section 6

Unlike the simplest asynchronous coupling techniques this structure ensures consistency between the surface hydrological states "seen" by the atmosphere and the vegetation. This is achieved by having a strong demarcation between the processes represented in TRIFFID and those represented in the MOSES 2 land-surface scheme. Specifically, MOSES 2 calculates instantaneous carbon fluxes (consistent with the modelled surface energy and water fluxes) using parameters provided by TRIFFID, whilst TRIFFID updates the vegetation and soil state (and associated parameters) using the accumulated fluxes passed from MOSES 2.

3 Vegetation Dynamics

At the core of TRIFFID are first order differential equations describing how the vegetation carbon density, C_v, and fractional coverage, ν, of a given PFT are updated based on the carbon balance of that PFT and on competition with other PFTs:

$$\frac{dC_v}{dt} = (1-\lambda)\,\Pi - \Lambda_l \qquad (1)$$

$$C_v \frac{d\nu}{dt} = \lambda \Pi \nu_* \left\{ 1 - \sum_j c_{ij} \nu_j \right\} - \gamma_\nu \nu_* C_v \quad (2)$$

where $\nu_* = \mathrm{MAX}\{\nu, 0.01\}$, and Π is the net primary productivity per unit vegetated area of the PFT in question (as calculated in the MOSES 2 land surface scheme). A fraction λ of this NPP is utilised in increasing the fractional coverage (equation 2), and the remainder increases the carbon content of the existing vegetated area (equation 1). Equation 1 therefore represents the local carbon balance as utilised in most terrestrial carbon cycle models. TRIFFID is unusual in that this is coupled to equation 2, which is based on the the Lotka-Volterra approach to intraspecies and interspecies competition (see for example Silvertown (1987)). Lotka-Volterra equations are used frequently in theoretical population dynamics but have not previously been applied in a DGVM. In order to do so here, we have replaced the usual population state variable of number density with the fractional area covered by the PFT, and driven increases in ν directly with NPP (via the first term on the righthandside of equation 2). Under most circumstances the variable ν_* is identical to the areal fraction, ν, but each PFT is "seeded" by ensuring that ν_* never drops below the "seed fraction" of 0.01.

The competition coefficients, c_{ij}, represent the impact of vegetation type "j" on the vegetation type of interest (type "i", although for clarity this subscript has been dropped from other variables in equations 1 and 2). These coefficients all lie between zero and unity, so that competition for space acts to reduce the growth of ν that would otherwise occur (i.e. it produces density-dependent litter production). Each PFT experiences "intraspecies" competition, with $c_{ii} = 1$ so that vegetation fraction is always limited to be less than one. Competition between natural PFTs is based on a tree-shrub-grass dominance heirachy, with dominant types "i" limiting the expansion of subdominant types "j" ($c_{ji} = 1$), but not vice-versa ($c_{ij} = 0$). However, the tree types (broadleaf and needleleaf) and grass types (C_3 and C_4) co-compete with competition coefficients dependent on their relative heights, h_i and h_j:

$$c_{ij} = \frac{1}{1 + \exp\{20\,(h_i - h_j)/(h_i + h_j)\}} \quad (3)$$

The form of this function ensures that the i^{th} PFT dominates when it is much taller, and the j^{th} PFT dominates in the opposite limit. The factor of 20 was chosen to give co-competition over a reasonable range of height differences. Some allowance is made for agricultural regions, from which the woody types (i.e. trees and grasses) are excluded, and C_3 and C_4 grasses are reinterpreted as "crops".

The λ partitioning coefficient in equations 1 and 2 is assumed to be piecewise linear in the leaf area index, with all of the NPP being used for growth for small LAI values, and all the NPP being used for "spreading" for large LAI values:

$$\lambda = \begin{cases} 1 & \text{for } L_b > L_{max} \\ \dfrac{L_b - L_{min}}{L_{max} - L_{min}} & \text{for } L_{min} < L_b \leq L_{max} \\ 0 & \text{for } L_b \leq L_{min} \end{cases} \quad (4)$$

where L_{max} and L_{min} are parameters describing the maximum and minimum leaf area index values for the given plant functional type, and L_b is the "balanced" LAI which would be reached if the plant was in "full leaf". The actual LAI depends on L_b and the phenological status of the vegetation type, which is updated as a function of temperature (see section 4).

Changes in vegetation carbon density, C_v, are related allometrically to changes in the balanced LAI, L_b. First, C_v is broken down into leaf, $\mathcal{L}$, root, $\mathcal{R}$, and total stem carbon, $\mathcal{W}$:

$$C_v = \mathcal{L} + \mathcal{R} + \mathcal{W} \quad (5)$$

Then each of these components are related to L_b. Root carbon is set equal to leaf carbon, which is itself linear in LAI, and total stem carbon is related to L_b by a power law (Enquist *et al* (1998)):

$$\mathcal{L} = \sigma_l L_b \tag{6}$$

$$\mathcal{R} = \mathcal{L} \tag{7}$$

$$\mathcal{W} = a_{wl} L_b^{5/3} \tag{8}$$

Here σ_l is the specific leaf carbon density (kg C m^{-2} LAI^{-1}) of the vegetation type, and a_{wl} is a PFT-dependent parameter in the power law relating LAI and total stem biomass. Recent work by Enquist *et al* (1998) suggests that 4/3 (rather than 5/3) may be a more appropriate power to use in the next version of TRIFFID. Values of canopy height, h, are directly from $\mathcal{W}$ as described in section 6.

The local litterfall rate, Λ_l, in equation 1, consists of contributions from leaf, root and stem carbon:

$$\Lambda_l = \gamma_l \mathcal{L} + \gamma_r \mathcal{R} + \gamma_w \mathcal{W} \tag{9}$$

where γ_l, γ_r and γ_w are turnover rates (yr^{-1}) for leaf, root and stem carbon respectively. The leaf turnover rate is calculated to be consistent with the phenological module as described in section 4. The root turnover rate is set equal to the minimum leaf turnover rate $\gamma_0 = 0.25$ for all PFTs, but the total stem turnover is PFT-dependent to reflect the different fractions of woody biomass (see table 1). There is an additional litter contribution arising from large-scale disturbance which results in loss of vegetated area at the prescribed rate γ_ν, as represented by the last term on the righthandside of equation 2.

4 Leaf Phenology

Leaf mortality rates, γ_{lm}, for the tree-types are assumed to be a function of temperature, increasing from a minimum value of γ_0, as the leaf temperature drops below a threshold value, T_{off}:

$$\gamma_{lm} = \begin{cases} \gamma_0 & \text{for } T > T_{off} \\ \gamma_0 \{1 + 9 (T_{off} - T)\} & \text{for } T \leq T_{off} \end{cases} \tag{10}$$

where $T_{off} = 0°C$ for broadleaf trees and $T_{off} = -30°C$ for needleleaf trees (Woodward (1987)). The factor of 9 is such that the leaf turnover rate increases by a factor of 10 when the temperature drops 1°C below T_{off}. Equation 10 describes how leaf mortality varies with temperature, but it is not sufficient to produce realistic phenology. A new variable, p, is introduced which describes the phenological status of the vegetation:

$$L = p L_b \tag{11}$$

where L is the actual LAI of the canopy, and L_b is the balanced (or seasonal maximum) LAI as updated by TRIFFID via the inverse of equation 8. The phenological status, p, is updated on a daily basis assuming:

- leaves are dropped at a constant absolute rate ($\gamma_p L_b$) when the daily mean value of leaf turnover, as given by equation 10, exceeds twice its minimum value
- budburst occurs at the same rate when γ_{lm} drops back below this threshold, and "full leaf" is approached assymptotically thereafter:

$$\frac{dp}{dt} = \begin{cases} -\gamma_p & \text{for } \gamma_{lm} > 2\,\gamma_0 \\ \gamma_p\,\{1-p\} & \text{for } \gamma_{lm} \leq 2\,\gamma_0 \end{cases} \tag{12}$$

where $\gamma_p = 20$ yr^{-1}. The effective leaf turnover rate, γ_l, as used in equation 9, must also be updated to ensure conservation of carbon when phenological changes are occurring:

$$\gamma_l = \begin{cases} -\dfrac{dp}{dt} & \text{for } \gamma_{lm} > 2\,\gamma_0 \\ p\,\gamma_{lm} & \text{for } \gamma_{lm} \leq 2\,\gamma_0 \end{cases} \tag{13}$$

Taken together, equation 10, 12 and 13 amount to a "chilling-days" parametrization of leaf phenology. A similar approach may be taken for drought-deciduous phenology and for the cold-deciduous phenology of the other (non-tree) PFTs, but neither is included in this version of TRIFFID.

5 Soil Carbon

Soil carbon storage, C_s, is increased by the total litterfall, Λ_c, and reduced by microbial soil respiration, R_s, which returns CO_2 to the atmosphere:

$$\frac{dC_s}{dt} = \Lambda_c - R_s \tag{14}$$

In each gridbox, the total litterfall is made-up of the area-weighted sum of the local litterfall from each PFT (as given by equation 9), along with terms due to the large-scale disturbance rate, γ_ν, and PFT competition:

$$\Lambda_c = \sum_i \nu_i \left\{ \Lambda_{li} + \gamma_{\nu i}\, C_{vi} + \Pi_i \sum_j c_{ij}\,\nu_j \right\} \tag{15}$$

The competition term (last term on the righthand side of equation 15) is derived by imposing carbon conservation on the soil-vegetation system as described by equations 1, 2 and 14. It implies that the NPP of each PFT will be lost entirely as litter once the PFT occupies all of the space available to it (i.e. when $\sum_j c_{ij}\nu_j = 1$).

The rate of soil respiration, R_s, is dependent on the soil temperature, T_s, volumetric soil moisture concentration, Θ, and soil carbon content, C_s:

$$R_s = \kappa_s\, C_s\, f_\Theta\, f_T \tag{16}$$

where $\kappa_s = 5 \times 10^{-9}$ s^{-1} is the specific soil respiration rate at 25 ° C, and f_Θ and f_T are moisture and temperature dependent functions respectively. The latter is assumed to take the "Q10" form:

$$f_T = q_{10}^{0.1\,(T_s - 25)} \tag{17}$$

where T_s is the soil temperature in °C and $q_{10} = 2.0$. The moisture dependence is based on the model of McGuire *et al* (1992) in which the respiration rate increases with soil moisture content until an optimum value of moisture is reached. Thereafter the rate of respiration is reduced with further increases in soil moisture. The curves presented by McGuire *et al* (1992) were approximated by piecewise linear functions in order to minimise the number of additional soil variables required.

$$f_\Theta = \begin{cases} 1 - 0.8\,\{S - S_o\} & \text{for } S > S_o \\ 0.2 + 0.8\left\{\dfrac{S - S_w}{S_o - S_w}\right\} & \text{for } S_w < S \leq S_o \\ 0.2 & \text{for } S \leq S_w \end{cases} \tag{18}$$

Here S, S_w and S_o are the (unfrozen) soil moisture, the wilting soil moisture and the optimum soil moisture as a fraction of saturation:

$$S = \frac{\Theta}{\Theta_s} \tag{19}$$

$$S_w = \frac{\Theta_w}{\Theta_s} \tag{20}$$

$$S_o = 0.5\ \{1 + S_w\} \tag{21}$$

where Θ, Θ_s and Θ_w are the (unfrozen) soil moisture concentration, the saturation soil moisture concentration and the wilting soil moisture concentration respectively.

6 Updating Biophysical Parameters

In order to close the biophysical feedback loop (see figure 2), the land-surface parameters required by the MOSES 2 land-surface scheme (Cox *et al* (1999)) are recalculated directly from the LAI and canopy height of each PFT, each time the vegetation cover is updated. Values of canopy height, h, are derived by assuming a fixed ratio, a_{ws}, of total stem carbon, $\mathcal{W}$, to respiring stem carbon, $\mathcal{S}$:

$$\mathcal{W} = a_{ws}\,\mathcal{S} \tag{22}$$

where we assume $a_{ws} = 10.0$ for woody plants and $a_{ws} = 1.0$ for grasses (Friend *et al* (1993)). Combining with equations 8 and 63 enables canopy height to be diagnosed directly from the total stem biomass:

$$h = \frac{\mathcal{W}}{a_{ws}\,\eta_{sl}} \left\{ \frac{a_{wl}}{\mathcal{W}} \right\}^{1/b_{wl}} \tag{23}$$

The aerodynamic roughness lengths, which are used by MOSES 2 to calculate surface-atmosphere fluxes of heat, water, momentum and CO_2, are assumed to be directly proportional to this canopy height:

$$z_0 = \begin{cases} 0.05\,h & \text{for trees} \\ 0.10\,h & \text{for grasses and shrubs} \end{cases} \tag{24}$$

where z_0 is the roughness length for momentum. The roughness lengths for scalars (heat, water and CO_2) are taken to be 0.1 of this value.

The snow-free albedo of each vegetation tile, α_0, is calculated as a weighted sum of the soil albedo, $\alpha_0 0$, and a prescribed maximum canopy albedo, $\alpha_{0\infty}$:

$$\alpha_0 = \alpha_{00}\ \exp\{-k\,L\} + \alpha_{0\infty}\,(1 - \exp\{-k\,L\}) \tag{25}$$

where L is the LAI, $k = 0.5$ and $\exp\{-kL\}$ represents the fraction of the incident light which passes through to the soil surface. This simple albedo parametrization uses values of $\alpha_{0\infty} = 0.1$ for tree types, and $\alpha_{0\infty} = 0.2$ for grasses and shrubs. The soil albedo is a geographically varying field derived from the dataset of Wilson and Henderson-Sellers (1985). A similar equation is used to calculate the "cold deep-snow" albedo, but here both albedo parameters are PFT-dependent. We assume maximum snow albedos of $\alpha_{s0} = 0.3$ for trees, and $\alpha_{s0} = 0.8$ for shrubs and grasses. The prescribed minimum snow albedos are; $\alpha_{s\infty} = 0.15$ for the tree types, $\alpha_{s\infty} = 0.6$ for grass types and $\alpha_{s\infty} = 0.4$ for shrubs. In all cases these parameters were chosen to approximate the albedo values used by Cox *et al* (1999).

The canopy catchment capacity, c_m, which determines the amount of water which is freely available for evaporation from the surface, varies linearly with LAI:

$$c_m = 0.5 + 0.05\,L \tag{26}$$

where the offset of 0.5 represents puddling of water on the soil surface and interception by leafless plants. The other hydrological land-surface parameters required by MOSES 2 are PFT-dependent, but do not depend directly on LAI or canopy height in this version. Root density is taken to fall off exponentially with depth, such that it is e^{-2} of its surface value at a specified rootdepth (of 3.0m for broadleaf trees, 1.0m for needleleaf trees and 0.5m for grasses and shrubs). Roots are assumed to enhance the maximum surface infiltration rate for water by a factor of 4 for trees, and 2 for the other PFTs.

7 Spin-up Methodology

Soil carbon and forest area have timescales of order 1000 years to reach equilibrium which means it is not feasible to carry out this spin-up in the fully coupled GCM. However, it is still vital to reach a good approximation to the pre-industrial equilibrium. The contemporary carbon sink is only a small fraction of the gross carbon exchanges between the Earth's surface and the atmosphere, and any significant model drift could easily swamp this signal. With this in mind, TRIFFID was designed to be usable in both "equilibrium" and "dynamic" mode.

This flexibility relies on the numerical design of the model. The TRIFFID equations to update the plant fractional coverage and leaf area index are written to enable both "explicit" and "implicit" timestepping. Thus for example, the dynamical equation for leaf area index, L, can be represented by:

$$\frac{dL}{dt} = F(L) \tag{27}$$

where F is a non-linear function of L. An explicit scheme uses the beginning-of-timestep value, L_n, to calculate F, whilst a fully implicit scheme uses the end-of-timestep value, L_{n+1}. In general the update equation may be written:

$$\frac{\Delta L}{\Delta t} = F(L_n + f\Delta L) \tag{28}$$

where Δt is the model timestep and f is the "forward timestep weighting factor", which is 0 for an explicit scheme and 1 for a fully implicit scheme. Taylor expansion about L_n provides an algebraic update for L:

$$\Delta L = \frac{F(L_n)\,\Delta t}{1 - f\,F'(L_n)\,\Delta t} \tag{29}$$

where $F'(L_n)$ is the derivative of F with respect to L at $L = L_n$. For $f = 1$ and large timesteps this equation reduces to the Newton-Raphson algorithm for iteratively approaching the equilibrium given by $F(L) = 0$.

Each of the TRIFFID prognostic equations is written in the form represented by equation 29, which allows the model to be used in two distinct modes. In "equilibrium mode" TRIFFID is coupled asynchronously to the atmospheric model, with accumulated carbon fluxes passed from MOSES 2 typically every 5 or 10 years. On each TRIFFID call, the vegetation and soil variables are updated iteratively using an implicit scheme ($f = 1$) with a long internal timestep (10,000 years by default). Offline tests have shown that this approach is very effective in producing equilibrium states for the slowest variables (e.g. soil carbon and forest cover). In "dynamic mode", equation 29 is used with $f = 0$ and a timestep equal to the TRIFFID-GCM coupling period (typically 10 days).

Although the equilibrium mode is effective at bringing the slower components to equilibrium, it is often necessary to carry-out a subsequent dynamical TRIFFID run so as to allow the faster varying components (such as grasses) to come into equilibrium with the seasonally varying climate. During the pre-industrial spin-up of the HadCM3LC coupled climate-carbon cycle model (Cox *et al* (2000)) we completed a 60 year GCM run with TRIFFID in equilibrium mode (5 year coupling period) and

followed this by a GCM simulation of 90 years with TRIFFID in its dynamical mode (10 day coupling period). This was necessary to meet the rather stringent requirements of net carbon balance set to ensure that the current carbon sink was not swamped by model drift. For many other purposes (such as simulations of palaeoclimate-vegetation interactions) much shorter simulations should suffice (e.g. 20 years in equilibrium mode followed by 10 years in dynamical mode).

8 Further Reading

We have described the TRIFFID dynamic global vegetation model which has been coupled consistently to the Met Office/Hadley Centre GCM. TRIFFID has already been successfully used in coupled climate-carbon cycle simulations, where it reproduces the key features of the global vegetation distribution (Cox *et al* (2001)) and contributes to realistic variability in the global carbon cycle (Jones *et al* (submitted), Jones and Cox (in press)). Scenarios of future climate change computed with the coupled climate-carbon cycle model suggest that land carbon cycle feedbacks (from TRIFFID) could significantly accelerate global warming in the next century (Cox *et al* (2000)). Copies of these papers and reports can be obtained on request from the author.

References

Betts, R. A., P. M. Cox, S. E. Lee, and F. I. Woodward, 1997: Contrasting physiological and structural vegetation feedbacks in climate change simulations. *Nature*, **387**, 796–799.

Claussen, M., 1996: Variability of global biome patterns as a function of initial and boundary conditions in a climate model. *Climate Dynamics*, **12**, 371–379.

Collatz, G. J., J. T. Ball, C. Grivet, and J. A. Berry, 1991: Physiological and environmental regulation of stomatal conductance, photosynthesis and transpiration: A model that includes a laminar boundary layer. *Agric. and Forest Meteorol.*, **54**, 107–136.

——, M. Ribas-Carbo, and J. A. Berry, 1992: A coupled photosynthesis-stomatal conductance model for leaves of C_4 plants. *Aus. J. Plant Physiol.*, **19**, 519–538.

Cox, P. M., C. Huntingford, and R. J. Harding, 1998: A canopy conductance and photosynthesis model for use in a GCM land surface scheme. *Journal of Hydrology*, **212–213**, 79–94.

——, R. A. Betts, C. B. Bunton, R. L. H. Essery, P. R. Rowntree, and J. Smith, 1999: The impact of new land surface physics on the GCM simulation of climate and climate sensitivity. *Clim. Dyn.*, **15**, 183–203.

Cox, P., R. Betts, C. Jones, S. Spall, and I. Totterdell, 2000: Acceleration of global warming due to carbon–cycle feedbacks in a coupled climate model. *Nature*, **408**, 184–187.

——, ——, ——, ——, and ——, 2001: Modelling vegetation and the carbon cycle as interactive elements of the climate system. Technical Note 23, Hadley Centre, Met Office.

Enquist, B., J. Brown, and G. West, 1998: Allometric scaling of plant energetics and population density. *Nature*, **395**, 163–166.

Foley, J. A. et al., 1996: An integrated biosphere model of land surface processes, terrestrial carbon balance and vegetation dynamics. *Global Biogeochemical Cycles*, **10**(4), 603–628.

Friend, A. D., H. H. Shugart, and S. W. Running, 1993: A physiology-based model of forest dynamics. *Ecology*, **74**, 797–797.

Jacobs, C., 1994: *Direct impact of atmospheric CO_2 enrichment on regional transpiration*. PhD thesis, Wageningen Agricultural University.

Jones, C., and P. Cox, in press: Modelling the volcanic signal in the atmospheric CO_2 record. *Global Biogeochem. Cycles*.

——, M. Collins, P. Cox, and S. Spall, submitted: The carbon cycle response to ENSO: A coupled climate–Carbon cycle model study. *J. Clim.*

McGuire, A., J. Melillo, L. Joyce, D. Kicklighter, A. Grace, B. M. III, and C. Vorosmarty, 1992: Interactions between carbon and nitrogen dynamics in estimating net primary productivity for potential vegetation in North America. *Global Biogeochem. Cycles*, **6**, 101–124.

Post, W. M., and J. Pastor, 1996: LINKAGES - an individual-based forest ecosystem model. *Climatic Change*, **34**, 253–261.

Prentice, I., W. Cramer, S. P. Harrison, R. Leemans, R. A. Monserud, and A. M. Solomon, 1992: A global biome model based on plant physiology and dominance, soil properties and climate. *Journal of Biogeography*, **19**, 117–134.

Schulze, E. D., F. M. Kelliher, C. Korner, and J. Lloyd, 1994: Relationships among maximum stomatal conductance, ecosystem surface conductance, carbon assimilation rate, and plant nitrogen nutrition: a global ecology scaling exercise. *Annual Review of Ecological Systems*, **25**, 629–660.

Sellers, P., J. Berry, G. Collatz, C. Field, and F. Hall, 1992: Canopy reflectance, photosynthesis and transpiration, III. a reanalysis using enzyme kinetics - electron transport models of leaf physiology. *Remote Sensing of Environment*, **42**, 187–216.

——, D. Randall, C. Collatz, J. Berry, C. Field, D. Dazlich, C. Zhang, and G. Collelo, 1996: A revised land surface parameterisation (SiB2) for atmospheric GCMs. Part I: Model formulation. *Journal of Climate*, **9**, 676–705.

Silvertown, J., 1987: *Introduction to Plant Population Ecology*. Longman Scientific and Technical, second edition.

Wilson, M. F., and A. Henderson-Sellers, 1985: A global archive of land cover and soils data for use in general circulation climate models. *Journal of Climatology*, **5**, 119–143.

Woodward, F. I., T. M. Smith, and W. R. Emanuel, 1995: A global land primary productivity and phytogeography model. *Global Biogeochemical Cycles*, **9**, 471–490.

——, 1987: *Climate and Plant Distribution*. Cambridge University Press.

A Vegetation Carbon Fluxes

A.1 Basic Model Structure

Stomatal openings are the pathways through which both water and carbon dioxide are exchanged between vegetation and the atmosphere. Consequently, net leaf photosynthesis, A (mol CO_2 m^{-2} s^{-1}), and stomatal conductance to water vapour, g_s (m s^{-1}), are linked through:

$$A = \frac{g_s}{1.6\,R\,T_*}\,(c_c - c_i) \tag{30}$$

where R is the perfect gas constant, T_* (K) is the leaf surface temperature, and c_c and c_i (Pa) are the leaf surface and internal CO_2 partial pressures respectively. The factor of 1.6 accounts for the different molecular diffusivities of water and carbon dioxide. Leaf photosynthesis is known to be dependent on a number of environmental variables as well as the internal CO_2 concentration, c_i:

$$A = A(\vec{X}, c_i) \tag{31}$$

where $\vec{X}$ represents a general vector of environmental variables. Equations 30 and 31 contain three unknowns; A, g and c_i. The closure suggested by Jacobs (1994) is in MOSES (Cox *et al* (1998), Cox *et al* (1999)):

$$\left\{\frac{c_i - \Gamma}{c_c - \Gamma}\right\} = F_0 \left\{1 - \frac{D_*}{D_c}\right\} \tag{32}$$

where Γ is the internal partial pressure of CO_2 at which photosynthesis just balances photorespiration (the "photorespiration compensation point"), D_* is the humidity deficit at the leaf surface, and F_0 and D_c are vegetation specific parameters (see table 2). The leaf photosynthesis models represented by 31 are based on the work of Collatz *et al* (1991) and Collatz *et al* (1992) for C_3 and C_4 plants respectively. Details of these models are given below. However, an additional direct soil moisture dependence is introduced as suggested by Cox *et al* (1998):

$$A = A_p\,\beta \tag{33}$$

where A_p is the "potential" (non-moisture stressed) rate of net photosynthesis as given by the models described below, and β is the moisture stress factor:

$$\beta = \begin{cases} 1 & \text{for } \Theta > \Theta_c \\ \dfrac{\Theta - \Theta_w}{\Theta_c - \Theta_w} & \text{for } \Theta_w < \Theta \leq \Theta_c \\ 0 & \text{for } \Theta \leq \Theta_w \end{cases} \tag{34}$$

Here, Θ_c and Θ_w are the critical and wilting soil moisture concentrations respectively, and Θ is the mean soil moisture concentration in the rootzone.

Equations 30 to 34 represent a coupled model of stomatal conductance and leaf photosynthesis. Large-scale applications require an economical means of scaling the predicted leaf-level fluxes up to the canopy scale. The approach of Sellers *et al* (1992) is used here, in which the primary determinants of photosynthesis, mean incident photosynthetically active radiation (PAR), I_{par}, and the maximum rate of carboxylation of Rubisco, V_{max}, are assumed to be proportional throughout the plant canopy:

$$I_{par}(l) = I_{par}(0)\exp\{-k\,l\} \tag{35}$$

$$V_{max}(l) = V_{max}(0)\exp\{-k\,l\} \tag{36}$$

where (l) denotes values beneath l leaf layers, (0) denotes values at the top of the canopy, and $k = 0.5$ is the PAR extinction coefficient. This assumption ensures that the relative importance of each of

the photosynthesis limiting factors is the same at every depth in the canopy. As a consequence it is straightforward to integrate the leaf conductance and photosynthesis over the canopy leaf area index, L, to yield canopy conductance, g_c, net canopy photosynthesis, A_c, and (non-moisture stressed) canopy dark respiration, R_{dc}:

$$g_c = g\, f_{par} \tag{37}$$
$$A_c = A\, f_{par} \tag{38}$$
$$R_{dc} = R_d\, f_{par} \tag{39}$$

where g, A and R_d are the conductance, net photosynthesis and (non-moisture stressed) dark respiration rate of the top leaf layer and

$$f_{par} = \frac{1 - \exp\{-k\, L\}}{k} \tag{40}$$

Gross primary productivity, Π_G, is equivalent to the gross canopy photosynthesis:

$$\Pi_G = 0.012\, \{A_c + R_{dc}\, \beta\} \tag{41}$$

where the factor 0.012 converts from units of (mol CO_2 m^{-2} s^{-1}) to (kg C m^{-2} s^{-1}), and the second term in the brackets is the actual (moisture modified) canopy dark respiration. Net primary productivity, Π (kg C m^{-2} s^{-1}), is:

$$\Pi = \Pi_G - R_p \tag{42}$$

where R_p (kg C m^{-2} s^{-1}) is the total plant respiration. The calculation of R_p is described in subsection A.3.

A.2 Leaf Photosynthesis Models

The C_3 and C_4 photosynthesis models are based on the work of Collatz *et al* (1991) and Collatz *et al* (1992), as applied by Sellers *et al* (1996). In both cases the rate of gross leaf photosynthesis, W (mol CO_2 m^{-2} s^{-1}), is calculated in terms of three potentially limiting factors:

(i) W_c represents the rate of gross photosynthesis when the photosynthetic enzyme system (RuBP) is limiting:

$$W_c = \begin{cases} V_m \left\{ \dfrac{c_i - \Gamma}{c_i + K_c\,(1 + O_a/K_o)} \right\} & \text{for } C_3 \text{ plants} \\ V_m & \text{for } C_4 \text{ plants} \end{cases} \tag{43}$$

where V_m (mol CO_2 m^{-2} s^{-1}) is the maximum rate of carboxylation of Rubisco, O_a (Pa) is the partial pressure of atmospheric oxygen, and K_c and K_o (Pa) are Michaelis-Menten constants for CO_2 and O_2 respectively.

(ii) W_l is the light-limited rate of gross photosynthesis:

$$W_l = \begin{cases} 0.08\,(1 - \omega)\, I_{par} \left\{ \dfrac{c_i - \Gamma}{c_i + 2\Gamma} \right\} & \text{for } C_3 \text{ plants} \\ 0.04\,(1 - \omega)\, I_{par} & \text{for } C_4 \text{ plants} \end{cases} \tag{44}$$

where I_{par} is the incident photosynthetically active radiation (mol PAR photons m^{-2} s^{-1}) and ω is the leaf scattering coefficient for PAR. The coefficients of 0.08 and 0.04 represent the "quantum efficiency" of C_3 and C_4 plants respectively. We follow Collatz *et al* (1991) and Collatz *et al* (1992) in assuming $\omega = 0.15$ for C_3 plants, and $\omega = 0.17$ for C_4 plants.

(iii) W_e is the limitation associated with transport of the photosynthetic products for C_3 plants, but is the PEP-Carboxylase limitation for C_4 plants (Collatz *et al* (1992)):

$$W_e = \begin{cases} 0.5\, V_m & \text{for } C_3 \text{ plants} \\ 2 \times 10^4\, V_m\, \dfrac{c_i}{p_*} & \text{for } C_4 \text{ plants} \end{cases} \tag{45}$$

where p_* is the surface air pressure.

The actual rate of gross photosynthesis, W, is calculated as the smoothed minimum of these three limiting rates:

$$\beta_1 W_p^2 - W_p \{W_c + W_l\} + W_c W_l = 0 \tag{46}$$

$$\beta_2 W^2 - W \{W_p + W_e\} + W_p W_e = 0 \tag{47}$$

where W_p is the smoothed minimum of W_c and W_l, and $\beta_1 = 0.83$ and $\beta_2 = 0.93$ are "co-limitation" coefficients. The smallest root of each quadratic is selected. Finally (non-moisture stressed) net leaf photosynthesis, A_p, is calculated by subtracting the rate of dark respiration, R_d, from the gross photosynthetic rate, W:

$$A_p = W - R_d \tag{48}$$

The parameters R_d, V_m, K_o, K_c and Γ are all temperature dependent functions derived from Collatz *et al* (1991) for C_3 plants and Collatz *et al* (1992) for C_4 plants:

- V_m, (mol CO_2 m^{-2} s^{-1}) the maximum rate of carboxylation of Rubisco:

$$V_m = \frac{V_{max}\, f_T(2.0)}{[1 + \exp\{0.3\,(T_c - T_{upp})\}]\,[1 + \exp\{0.3\,(T_{low} - T_c)\}]} \tag{49}$$

where T_c is the leaf temperature in °C, T_{upp} and T_{low} are PFT-dependent parameters, and f_T is the standard "Q10" temperature dependence:

$$f_T(q_{10}) = q_{10}^{0.1\,(T_c - 25)} \tag{50}$$

The standard photosynthesis models of Collatz *et al* (1991) and Collatz *et al* (1992) assume specific values of T_{upp} and T_{low} for C_3 and C_4 plants respectively ($T_{low} \to -\infty$, $T_{upp} = 36$ °C for C_3 plants, and $T_{low} = 13$ °C, $T_{upp} = 45$ °C for C_4 plants). However, in order to capture the temperature responses of all terrestrial eceosystems, it is necessary to make these parameters more generally dependent on PFT (i.e. not just dependent on the photosynthetic pathway). Values of the values chosen are shown in table 2.

V_{max} (mol CO_2 m^{-2} s^{-1}) is assumed to be linearly dependent on the leaf nitrogen concentration, n_l (kg N (kg C)$^{-1}$):

$$V_{max} = \begin{cases} 0.0008\, n_l & \text{for } C_3 \text{ plants} \\ 0.0004\, n_l & \text{for } C_4 \text{ plants} \end{cases} \tag{51}$$

The constants of proportionality are derived from Schulze *et al* (1994) by assuming that dry matter is 40 % carbon by mass and that the maximum rate of photosynthesis is approximately equal to $0.5V_{max}$ for C_3 plants and approximately equal to V_{max} for C_4 plants.

- Γ, (Pa) the photorespiration compensation point:

$$\Gamma = \begin{cases} \dfrac{O_a}{2\,\tau} & \text{for } C_3 \text{ plants} \\ 0 & \text{for } C_4 \text{ plants} \end{cases} \tag{52}$$

where τ is the Rubisco specificity for CO_2 relative to O_2:

$$\tau = 2600\, f_T(0.57) \tag{53}$$

- K_c and K_o (Pa), Michaelis-Menten constants for CO_2 and O_2:

$$K_c = 30\, f_T(2.1) \tag{54}$$
$$K_o = 3 \times 10^4\, f_T(1.2) \tag{55}$$

- The rate of dark respiration, R_d (mol CO_2 m^{-2} s^{-1}) is also assumed to have a "Q10" temperature dependence, with a constant of proportionality which depends on V_{max} (i.e. leaf nitrogen concentration):

$$R_d = \begin{cases} 0.015\, V_{max}\, f_T(2.0) & \text{for } C_3 \text{ plants} \\ \\ 0.025\, V_{max}\, f_T(2.0) & \text{for } C_4 \text{ plants} \end{cases} \tag{56}$$

  Note: this differs from the dark respiration rate used by Cox *et al* (1998) and Cox *et al* (1999), which was taken to be directly proportional to V_m as given by 49.

A.3 Plant Respiration

Plant respiration, R_p, is split into maintenance and growth respiration:

$$R_p = R_{pm} + R_{pg} \tag{57}$$

Growth respiration is assumed to be a fixed fraction of the net primary productivity, thus:

$$R_{pg} = r_g\, \{\Pi_G - R_{pm}\} \tag{58}$$

where Π_G is the gross primary productivity, and the growth respiration coefficient is set to $r_g = 0.25$ for all plant functional types. Leaf maintenance respiration is equivalent to the moisture modified canopy dark respiration, βR_{dc}, while root and stem respiration is assumed to be independent of soil moisture, but to have the same dependences on nitrogen content and temperature. Thus total maintenance respiration is given by:

$$R_{pm} = 0.012\, R_{dc} \left\{ \beta + \frac{(N_r + N_s)}{N_l} \right\} \tag{59}$$

where N_l, N_s and N_r are the nitrogen contents of leaf, stem and root, and the factor of 0.012 converts from (mol CO_2 m^{-2} s^{-1}) to (kg C m^{-2} s^{-1}). The nitrogen contents are given by:

$$N_l = n_l\, \sigma_l\, L \tag{60}$$
$$N_r = \mu_{rl}\, n_l\, \mathcal{R} \tag{61}$$
$$N_s = \mu_{sl}\, n_l\, \mathcal{S} \tag{62}$$

where n_l is the mean leaf nitrogen concentration (kg N (kg C)$^{-1}$), $\mathcal{R}$ and $\mathcal{S}$ are the carbon contents of respiring root and stem, L is the canopy leaf area index and σ_l (kg C m^{-2}) is the specific leaf density. The nitrogen concentrations of root and stem are assumed to be fixed (functional type dependent) multiples, μ_{rl} and μ_{sl}, of the mean leaf nitrogen concentration. In this study, we assume $\mu_{rl} = 1.0$ for all PFTS, $\mu_{sl} = 0.1$ for woody plants (trees and shrubs) and $\mu_{sl} = 1.0$ for grasses. The respiring stemwood is calculated using a "pipemodel" approach in which live stemwood is proportional to leaf area, L, and canopy height, h:

$$\mathcal{S} = 0.01\, h\, L \tag{63}$$

The constant of proportionality is approximated from Friend *et al* (1993).

Parameter	Units	Broadleaf Tree	Needleleaf Tree	C_3 Grass	C_4 Grass	Shrub
a_{wl}	kg C m^{-2}	0.650	0.650	0.005	0.005	0.100
γ_ν	yr^{-1}	0.004	0.004	0.100	0.100	0.030
γ_w	yr^{-1}	0.010	0.010	0.200	0.200	0.050
γ_0	yr^{-1}	0.250	0.250	0.250	0.250	0.250
L_{max}		9	9	4	4	4
L_{min}		3	3	1	1	1

Table 1: PFT-specific parameters for the dynamic vegetation component of TRIFFID. The values of a_{wl} were chosen to give realistic maximum biomass densities from equation 8. The other parameters were chosen largely by model calibration in offline tests, but realistic constraints were applied. For example, the large-scale disturbance rate, γ_ν, should yield realistic effective plant lifetimes, and the total stemwood turnover rate, γ_w, should reflect the differing percentages of wood amongst the PFTs. The minimum leaf turnover rate, γ_0, was set uniform across the PFTs for simplicity. This value is also used to specify the turnover of root biomass.

Parameter	Units	Broadleaf Tree	Needleleaf Tree	C_3 Grass	C_4 Grass	Shrub
$n_l(0)$	kg N (kg C)$^{-1}$	0.040	0.030	0.060	0.030	0.030
σ_l	kg C m^{-2} LAI^{-1}	0.0375	0.100	0.025	0.050	0.050
F_0		0.875	0.875	0.900	0.800	0.900
D_c	kg $(kg)^{-1}$	0.090	0.060	0.100	0.075	0.100
T_{low}	°C	0	-5	0	13	0
T_{upp}	°C	36	31	36	45	36

Table 2: PFT-specific parameters used in the MOSES 2 calculation of vegetation carbon fluxes. The values for top-leaf nitrogen concentration, $n_l(0)$, and specific leaf density, σ_l, are derived from the survey of Schulze *et al* (1994), which suggests that $n_l(0)\,\sigma_l = 1.5 \times 10^{-3}$ kg N m^{-2} LAI^{-1} for broadleaf plants, and $n_l(0)\,\sigma_l = 3 \times 10^{-3}$ kg N m^{-2} LAI^{-1} for needleleaf plants. Values of the maximum ratio of internal to external CO_2, F_0, and the critical humidity deficit, D_c, are chosen to give realistic maxima and humidity dependences for the canopy conductance (see for example, Cox *et al* (1998)). The lower and upper temperatures for photosynthesis, T_{low} and T_{upp} are consistent with the values prescribed by Collatz *et al* (1991) and Collatz *et al* (1992), except for the introduction of a finite lower bound for the C_3 plants, and the shift of the V_m curve for needleleaf trees by -5°C.

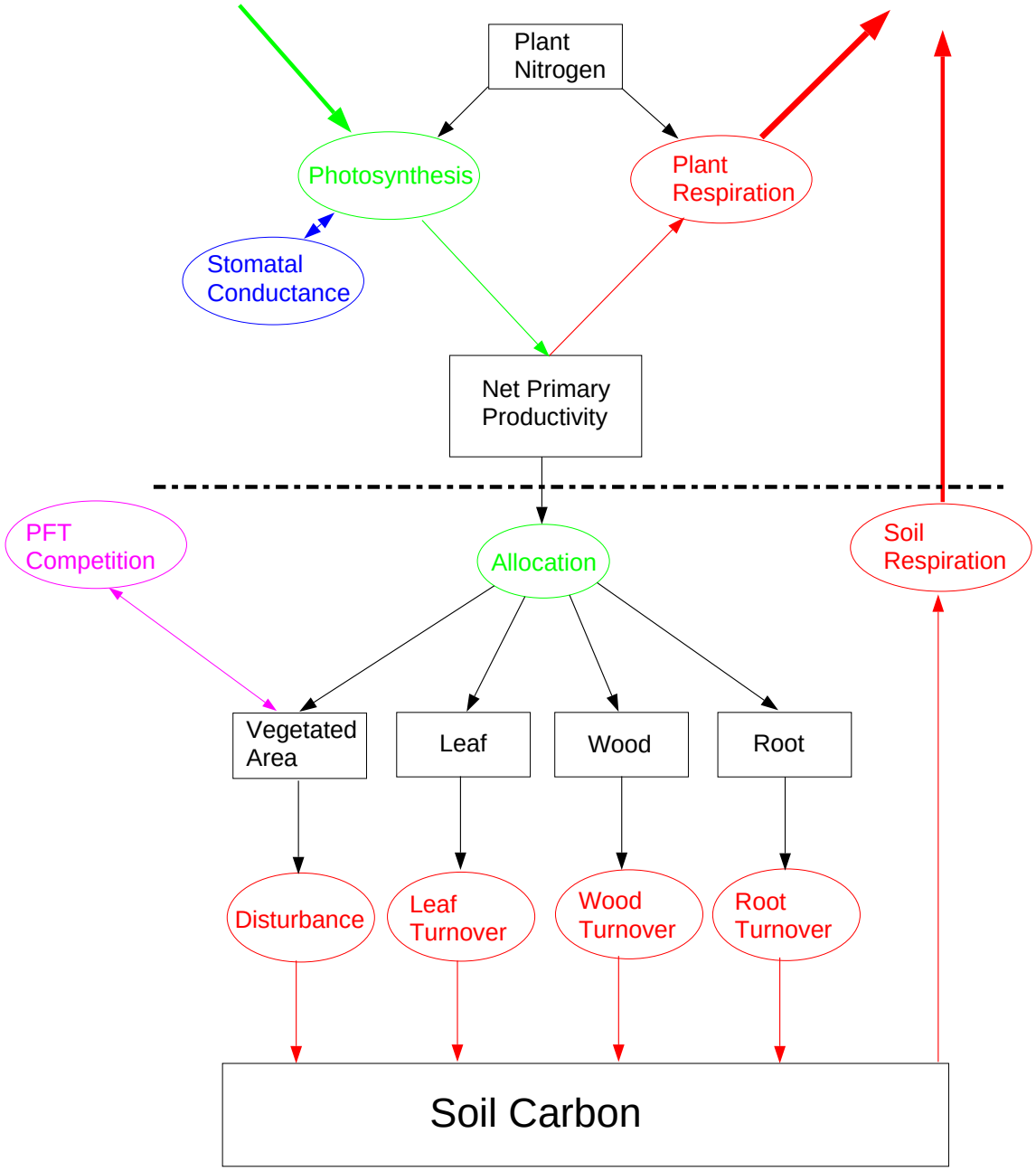

Figure 1: Schematic showing TRIFFID carbon flows for each vegetation type. Processes above the dotted line are fluxes calculated in the MOSES 2 land surface scheme every atmospheric model timestep ($\approx$ 30 minutes). In dynamic mode, TRIFFID updates the vegetation and soil carbon every 10 days using time-averages of these fluxes.

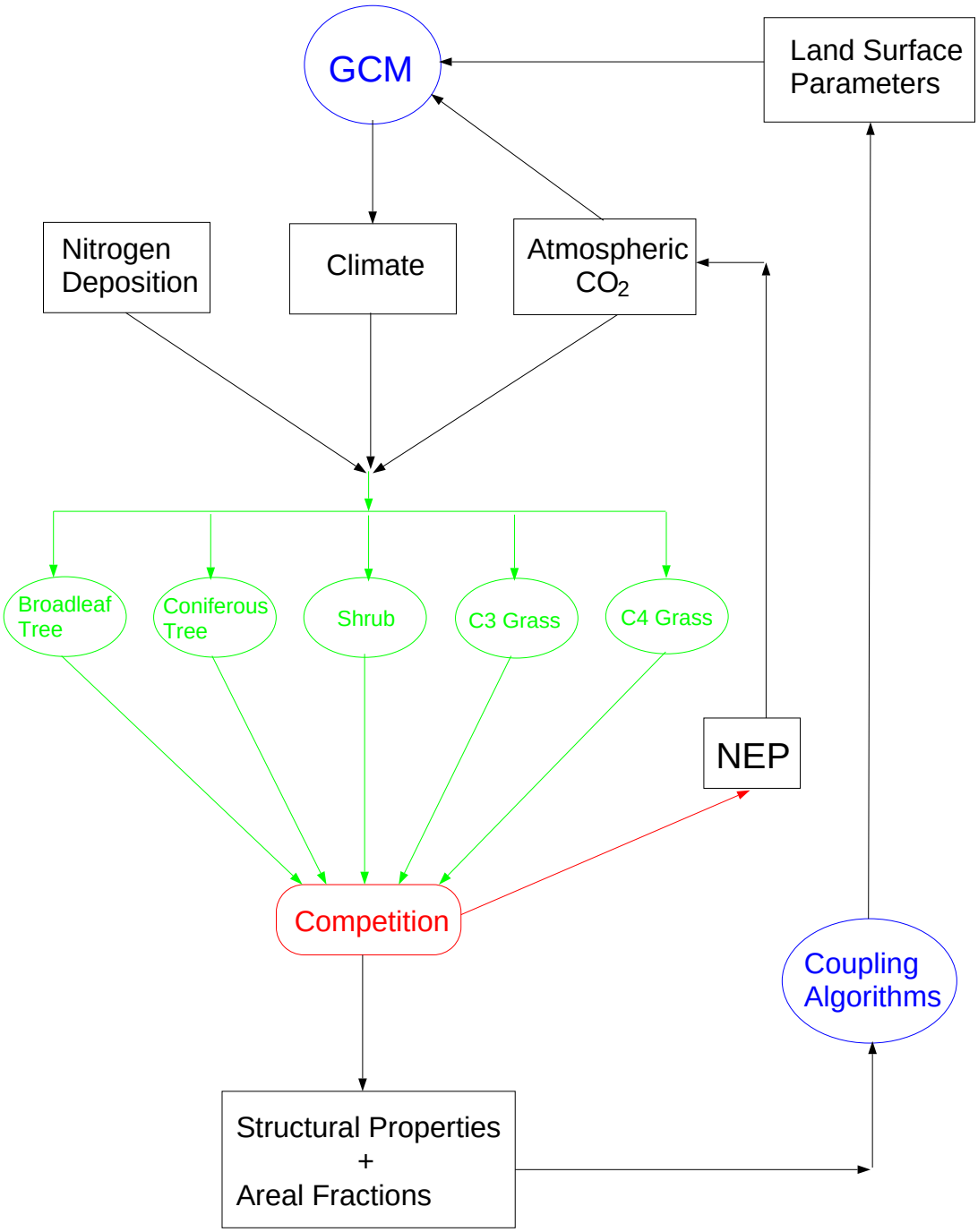

Figure 2: Schematic showing the coupling between TRIFFID and the GCM. Changes in the distribution and structure of the five plant functional types can provide a feedback to climate via two routes. The vegetation determines the biophysical land-surface parameters (e.g. albedo, roughness length, stomatal conductance) which in turn affect the land-atmosphere fluxes of heat, water and momentum. In addition, changes in the carbon stored in vegetation and soil (as measured by the net ecosystem productivity, "NEP") can change the evolution of atmospheric CO_2 and thus the climate through the greenhouse effect. For completeness nitrogen deposition is also shown as a driver for vegetation change, although this version of TRIFFID does not include an interactive nitrogen cycle.